Asian Journal of Chemistry; Vol. 37, No. 6 (2025), 1257-1265

ASIAN JOURNAL OF CHEMISTRY

https://doi.org/10.14233/ajchem.2025.33249

Novel 5-((Phenylimino)methyl)-1,2,4-triazol-3-one Derivatives: Synthesis, Anticancer Potential and Molecular Docking Insights

RAJITHA BALAVANTHAPU* and GIRIJA SASTRY VEDULA

Department of Chemistry, Andhra University, Visakhapatnam-530003, India

*Corresponding author: E-mail: rajitha.mpharm@gmail.com

Received: 23 December 2024; *Accepted*: 31 March 2025; *Published online*: 27 May 2025; AJC-21995

In this study, a series of substituted 5-((phenylimino)methyl)-2,4-dihydro-3*H*-1,2,4-triazol-3-one derivatives (**5a-o**) were synthesized and evaluated for their anticancer activity against various human cancer cell lines, including A549 (non-small cell lung cancer), HCT-116 (colorectal cancer) and PANC-1 (pancreatic cancer). The compounds were synthesized through a multi-steps process involving the preparation of ethyl β-*N*-Boc-oxalamidrazone, followed by cyclization to form ethyl 5-oxo-4,5-dihydro-1*H*-1,2,4-triazole-3-carboxylate, reduction to yield 5-oxo-4,5-dihydro-1*H*-1,2,4-triazole-3-carbaldehyde and subsequent condensation with various substituted anilines to obtain the final derivatives. Structures of the compounds were confirmed by ^{1}H NMR, ^{13}C NMR and high-resolution mass (HRMS) spectral methods. Molecular docking studies targeting epidermal growth factor receptor (EGFR) and cyclin-dependent kinase 4 (CDK4) revealed that certain derivatives, particularly those with electron-withdrawing groups like -NO_2, -OH and -CF_3, exhibited strong binding affinities, suggesting potential as inhibitors of these targets. *In vitro* cytotoxicity assays showed significant antiproliferative effects, with compound **5h** (4-CF_3) exhibiting the highest potency against A549 (IC_{50}: 7.80 ± 3.06 μM) and PANC-1 (IC_{50}: 8.75 ± 1.86 μM). Compound **5j** (3,4-$(OCH_3)_2$) demonstrated notable activity against A549 (IC_{50}: 5.96 ± 1.02 μM). Structure activity relationship analysis indicated that electron-donating groups generally enhanced activity, while electron-withdrawing groups had varying effects based on their position. These findings highlight the potential of these derivatives as lead compounds for anticancer drug development. Further optimization and *in vivo* studies are needed to fully explore their therapeutic potential.

Keywords: 1,2,4-Triazoles, Anticancer activity, Molecular docking, EGFR, CDK.

INTRODUCTION

Cancer, characterized by its life-threatening nature and uncontrolled proliferation, represents a significant global health challenge [1]. Although chemotherapy remains a standard treatment for targeting and eradicating rapidly dividing cancer cells, its lack of specificity results in collateral damage to healthy tissues, leading to adverse side effects. This non-selective toxicity underscores the urgent need for the development of novel anticancer agents that can more precisely target cancer cells while minimizing harm to normal tissues [2].

Targeted therapies aim to selectively eliminate cancer cells while minimizing damage to healthy tissues, thereby enhancing treatment precision and reducing adverse effects [3]. The 1,2,4-triazole nucleus is recognized as a highly versatile and promising scaffold for the development of novel anticancer agents. Its structural diversity allows for the incorporation of various substituents, facilitating the development of compounds with optimized properties [4]. 1,2,4-Triazole ring functions as a bio-isostere in medicinal chemistry, effectively substituting traditional functional groups to enhance the pharmacological profiles of the resulting molecules [5]. This substitution represents a significant advancement in pharmaceutical research.

Drugs like anastrozole and letrozole (Fig. 1), which are widely used and effective in treating hormone receptor-positive breast cancer, demonstrate the importance of the 1,2,4-triazole framework [6]. This study builds upon recent advancements that have demonstrated the efficacy of 1,2,4-triazole derivatives against multiple cancer-related targets, such as thymidine phosphorylase [7,8], aromatase [9], VEGFR [10-12], EGFR [13], topoisomerase [14,15] and tubulin polymerization [16,17]. These studies highlight the potential of scaffold in anticancer therapy, providing a strong foundation for further exploration.

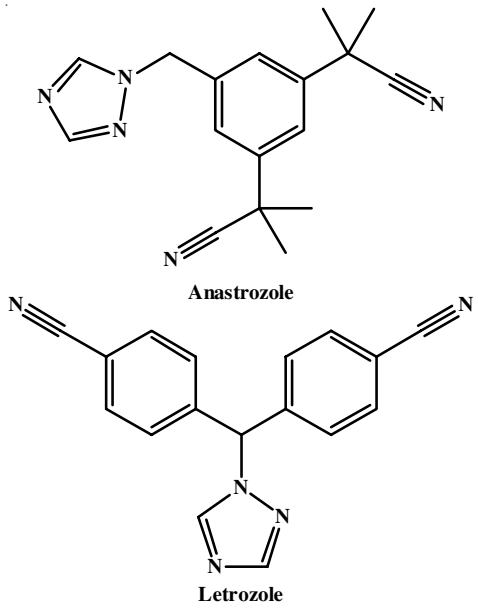

Fig. 1. Structures of anticancer drugs containing 1,2,4-triazole pharmacophore

These reports suggest that they possess the capacity to precisely target and interfere with critical pathways required for the proliferation of cancer cells. Moreover, compounds containing triazoles can surmount drug resistance, a significant barrier to cancer treatment. Certain compounds have advantageous pharmacokinetic characteristics, which increase their potential as effective, anticancer drugs [18,19]. Overall, the 1,2,4-triazole scaffold demonstrates significant potential for improving cancer treatment and patient outcomes.

The structural diversity, capacity to interact with multiple biological targets and favourable pharmacokinetic properties of the 1,2,4-triazole scaffold make it a promising platform for drug development. This study hypothesizes that targeted modifications of the 1,2,4-triazole scaffold with specific substituents will enhance its reactivity and selectivity against various cancer types. The primary objective is to design, synthesize and evaluate a series of novel 1,2,4-triazole derivatives, focusing on their anticancer activity. To elucidate the mechanisms underlying their activity, molecular docking studies were conducted to assess the interactions between the synthesized derivatives and key cancer targets, specifically EGFR and CDK-4. This approach aims to identify lead compounds with optimized therapeutic potential, advancing the scaffold's application in cancer therapy.

EXPERIMENTAL

All synthetic-grade chemicals and solvents used were purchased from Sigma-Aldrich, India, without further purification. The reaction was monitored using Merck-precoated aluminium TLC plates coated with silica gel 60 F_{254}. Remi electronic melting point equipment determined melting points. The ^{1}H and ^{13}C NMR spectra were collected using a Bruker DRX instrument and the chemical shift values were reported in ppm relative to the internal standard, tetramethyl silane. The HRMS spectra were collected using a Waters Xevo Q-Tof Mass spectrometer.

Synthesis: The synthetic scheme for the designed substituted 5-((phenylimino)methyl)-2,4-dihydro-3*H*-1,2,4-triazol-3-one (**5a-o**) is depicted in **Scheme-I** and the detailed procedure for the synthesis enumerated below:

Synthesis of ethyl β-*N*-Boc-oxalamidrazone (2): Thiooxamic acid ethyl ester (**6**, 1.82 g, 13.7 mmol) and Boc-hydrazine (1.81 g, 13.7 mmol) were dissolved in 10 mL of EtOH in a single-necked round-bottomed flask. The reaction mixture was stirred for 24 h. The precipitate was filtered, washed with

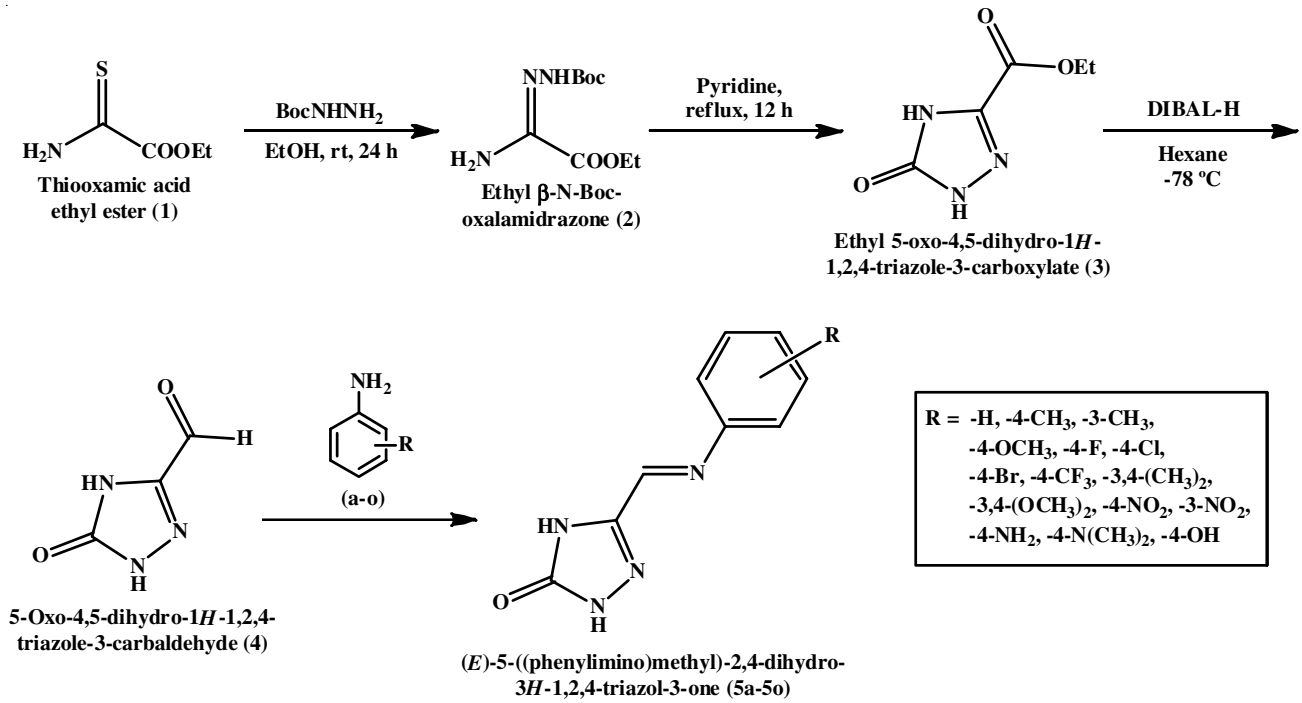

Scheme-I: Scheme of synthesis for substituted 5-((phenylimino)methyl)-2,4-dihydro-3*H*-1,2,4-triazol-3-one (**5a-o**)

10 mL of ethanol and air-dried, resulting in the production of ethyl β-*N*-Boc-oxalamidrazone **(2)** [20].

Synthesis of ethyl 5-oxo-4,5-dihydro-1*H*-1,2,4-triazole-3-carboxylate (3): Ethyl β-N-Boc-oxalamidrazone (**2**, 1 mmol) was mixed with pyridine (1 mmol) in a round-bottom flask equipped with a reflux condenser for a thermal cyclization reaction. The reaction mixture was heated and refluxed for 12 h. After the reaction was finished, the mixture was left to cool down to room temperature. The final product, ethyl 5-oxo-4,5-dihydro-1*H*-1,2,4-triazole-3-carboxylate (**3**), was obtained by a conventional acid workup method and extracted using ethyl acetate [20].

Synthesis of 5-oxo-4,5-dihydro-1*H*-1,2,4-triazole-3-carbaldehyde (4): Ethyl 5-oxo-4,5-dihydro-1*H*-1,2,4-triazole-3-carboxylate (0.7 g, 3.0 mmol) was dissolved in hexane (10 mL) and cooled to -78 ºC. A separate flask was charged with DIBAL-H (0.01 M in hexane, 3.0 mmol) and also cooled to -78 ºC. The DIBAL-H solution was transferred *via* cannula over 20-25 min then stirred at -78 ºC for 1 h. The reaction mixture was quenched by adding MeOH (10mL) and stirred at -78 ºC for 15 min. The cold solution was transferred to a 2L flask containing a saturated Rochelle salt solution (10 mL) and stirred for 30 min. The aqueous phase was separated and extracted further with hexane (20 mL). The combined org layers were washed with brine (10 mL), dried ($MgSO_4$), filtered and concentrated to provide the product [21].

General procedure for the synthesis of substituted 5-((phenylimino)methyl)-2,4-dihydro-3*H*-1,2,4-triazol-3-one (5a-o): 5-Oxo-4,5-dihydro-1*H*-1,2,4-triazole-3-carbaldehyde (**4**) dissolved in DCM (20 mL) stirred with pyrrolidine (10 mol%). Then the reaction mixture refluxed at 50 ºC for 4 h. Then the reaction mass was quenched with acetic acid solution, extracted with three equal portions of ethyl acetate and washed with brine solution. The ethyl acetate layer was evaporated under vacuum and the final product subjected to column chromatography to isolate the pure compounds (**5a-o**) (**Scheme-I**) [22].

(*E*)-5-((Phenylimino)methyl)-2,4-dihydro-3*H*-1,2,4-triazol-3-one (5a): White solid; yield: 80%; m.p.: 168-170 ºC; ^{1}H NMR (500 MHz, chloroform-d_6) δ ppm: 11.37 (s, 1H), 9.02 (s, 1H), 7.76 (s, 1H), 7.31 (dd, *J* = 8.0, 6.7 Hz, 2H), 7.17-7.10 (m, 1H), 7.09 (dd, *J* = 8.2, 1.4 Hz, 2H). ^{13}C NMR (125 MHz, chloroform-d_6) δ ppm: 156.47, 152.39, 146.55, 142.03, 129.81, 124.42, 121.77. HRMS: *m/z*: For $C_9H_8N_4O$ ([M + H]$^+$): 189.0714, found 189.0711.

(*E*)-5-((*p*-Tolylimino)methyl)-2,4-dihydro-3*H*-1,2,4-triazol-3-one (5b): White solid; yield: 72%; m.p.: 193-194 ºC; ^{1}H NMR (500 MHz, chloroform-d_6) δ ppm: 11.41 (s, 1H), 9.00 (s, 1H), 7.74 (s, 1H), 7.18 (d, *J* = 7.7 Hz, 2H), 7.11 (d, *J* = 7.8 Hz, 2H), 2.41 (s, 3H). ^{13}C NMR (125 MHz, chloroform-d_6) δ ppm: 23.30, 122.46, 128.84, 136.52, 142.90, 147.54, 150.73, 157.41. HRMS: *m/z*: For $C_{10}H_{10}N_4O$ ([M + H]$^+$): 203.0852, found 203.0849.

(*E*)-5-((*m*-Tolylimino)methyl)-2,4-dihydro-3*H*-1,2,4-triazol-3-one (5c): White solid; yield: 79%; m.p.: 191-192 ºC; ^{1}H NMR (500 MHz, chloroform-d_6) δ ppm: 11.39 (s, 1H), 8.97 (s, 1H), 7.72 (s, 1H), 7.29 (t, *J* = 7.6 Hz, 1H), 7.04 (dd, *J* = 7.6, 1.7 Hz, 1H), 7.01-6.95 (m, 1H), 6.94 (d, *J* = 2.2 Hz, 1H), 2.37 (s, 3H); ^{13}C NMR (125 MHz, chloroform-d_6) δ ppm: 22.86, 121.23, 122.96, 124.71, 130.87, 139.93, 142.90, 147.54, 151.24, 155.67. HRMS: *m/z*: For $C_{10}H_{10}N_4O$ ([M + H]$^+$): 203.0852, found 203.0849.

(*E*)-5-(((4-Methoxyphenyl)imino)methyl)-2,4-dihydro-3*H*-1,2,4-triazol-3-one (5d): White solid; yield: 80%; m.p.: 206-207 ºC; ^{1}H NMR (500 MHz, chloroform-d_6) δ ppm: 11.41 (s, 1H), 8.98 (s, 1H), 7.70 (s, 1H), 7.17 (d, *J* = 8.0 Hz, 2H), 6.89 (d, *J* = 8.1 Hz, 2H), 3.72 (s, 3H). ^{13}C NMR (125 MHz, chloroform-d_6) δ ppm: 56.79, 115.86, 124.92, 142.17, 146.31, 147.83, 156.16, 160.59. HRMS: *m/z*: For $C_{10}H_{10}N_4O_2$ ([M + H]$^+$): 219.0908, found 219.0905.

(*E*)-5-(((4-Fluorophenyl)imino)methyl)-2,4-dihydro-3*H*-1,2,4-triazol-3-one (5e): White solid; yield: 69%; m.p.: 159-160 ºC; ^{1}H NMR (500 MHz, chloroform-d_6) δ ppm: 11.48 (s, 1H), 9.06 (s, 1H), 7.72 (s, 1H), 7.20 (dd, *J* = 7.8, 3.4 Hz, 2H), 7.07 (dd, *J* = 10.2, 7.9 Hz, 2H). ^{13}C NMR (125 MHz, chloroform-d_6) δ ppm: 117.44, 117.62, 122.93, 123.00, 138.98, 145.07, 146.57, 146.62, 154.44, 158.87, 160.85. HRMS: *m/z*: For $C_9H_7FN_4O$ ([M + H]$^+$): 207.0598, found 207.0592.

(E)-5-(((4-Chlorophenyl)imino)methyl)-2,4-dihydro-3*H*-1,2,4-triazol-3-one (5f): White solid; yield: 71%; m.p.: 164-165 ºC; ^{1}H NMR (500 MHz, chloroform-d_6) δ ppm: 11.44 (s, 1H), 9.04 (s, 1H), 7.70 (s, 1H), 7.44 (d, *J* = 8.0 Hz, 2H), 7.20 (d, *J* = 8.0 Hz, 2H). ^{13}C NMR (125 MHz, chloroform-d_6) δ ppm: 123.98, 130.58, 131.81, 142.61, 147.83, 151.74, 155.97. HRMS: *m/z*: For $C_9H_7ClN_4O$ ([M + H]$^+$): 224.0336, found 224.0331.

(*E*)-5-(((4-Bromophenyl)imino)methyl)-2,4-dihydro-3*H*-1,2,4-triazol-3-one (5g): Off-white solid; yield: 76%; m.p.: 173-174 ºC; ^{1}H NMR (500 MHz, chloroform-d_6) δ ppm: 11.41 (s, 1H), 9.06 (s, 1H), 7.74 (s, 1H), 7.49 (d, *J* = 8.1 Hz, 2H), 7.27 (d, *J* = 8.1 Hz, 2H). ^{13}C NMR (125 MHz, chloroform-d_6) δ ppm: 117.02, 124.71, 131.59, 139.71, 145.36, 150.29, 153.72. HRMS: *m/z*: For $C_9H_7BrN_4O$ ([M + H]$^+$): 267.9712, found 267.9708.

(*E*)-5-(((4-(Trifluoromethyl)phenyl)imino)methyl)-2,4-dihydro-3*H*-1,2,4-triazol-3-one (5h): White solid; yield: 79%; m.p.: 182-183 ºC; ^{1}H NMR (500 MHz, chloroform-d_6) δ ppm: 11.44 (s, 1H), 9.08 (s, 1H), 7.78 (s, 1H), 7.64 (dq, *J* = 10.9, 1.5 Hz, 2H), 7.41 (d, *J* = 10.5 Hz, 2H). ^{13}C NMR (125 MHz, chloroform-d_6) δ ppm: 120.43, 122.61, 123.25, 123.28, 123.32, 123.36, 124.78, 126.96, 127.49, 127.53, 127.57, 127.61, 128.14, 128.40, 128.66, 128.92, 139.71, 144.86, 151.02, 153.72. HRMS: *m/z*: For $C_{10}H_7F_3N_4O$ ([M + H]$^+$): 257.0653, found 257.0649.

(*E*)-5-(((3,4-Dimethylphenyl)imino)methyl)-2,4-dihydro-3*H*-1,2,4-triazol-3-one (5i): White solid; yield: 85%; m.p.: 211-212 ºC; ^{1}H NMR (500 MHz, chloroform-d_6) δ ppm: 11.42 (s, 1H), 8.97 (s, 1H), 7.67 (s, 1H), 7.12 (dd, *J* = 7.8, 2.2 Hz, 1H), 7.01 (dd, *J* = 7.7, 1.2 Hz, 1H), 6.95 (d, *J* = 2.2 Hz, 1H), 2.26 (s, 3H), 2.20 (s, 3H). ^{13}C NMR (125 MHz, chloroform-d_6) δ ppm: 19.38, 20.40, 120.24, 120.94, 130.58, 135.51, 138.19, 142.17, 147.54, 149.49, 155.66. HRMS: *m/z*: For $C_{11}H_{12}N_4O$ ([M + H]$^+$): 217.1037, found 217.1035.

(*E*)-5-(((3,4-Dimethoxyphenyl)imino)methyl)-2,4-dihydro-3*H*-1,2,4-triazol-3-one (5j): White solid; yield: 78%;

m.p.: 228-229 ºC; ^{1}H NMR (500 MHz, chloroform-d_6) δ ppm: 11.39 (s, 1H), 9.04 (s, 1H), 7.70 (s, 1H), 6.98 (dd, *J* = 8.2, 2.1 Hz, 1H), 6.92-6.87 (m, 2H), 3.82 (s, 3H), 3.74 (s, 3H). ^{13}C NMR (125 MHz, chloroform-d_6) δ ppm: 55.93, 56.79, 106.22, 113.83, 118.04, 139.71, 143.64, 147.54, 150.00, 151.96, 155.46. HRMS: *m/z*: For $C_{11}H_{12}N_4O_3$ ([M + H]$^+$): 248.0985, found 248.0981.

(*E*)-5-(((4-Nitrophenyl)imino)methyl)-2,4-dihydro-3*H*-1,2,4-triazol-3-one (5k): Light yellow solid; yield: 72%; m.p.: 159-160 ºC; ^{1}H NMR (500 MHz, chloroform-d_6) δ ppm: 11.56 (s, 1H), 9.08 (s, 1H), 8.15 (d, *J* = 8.7 Hz, 2H), 7.81 (s, 1H), 7.35 (d, *J* = 8.6 Hz, 2H). ^{13}C NMR (125 MHz, chloroform-d_6) δ ppm: 121.73, 125.28, 140.43, 145.14, 147.54, 155.66, 158.43. HRMS: *m/z*: For $C_9H_7N_5O_3$ ([M + H]$^+$): 234.0597, found 234.0592.

(*E*)-5-(((3-Nitrophenyl)imino)methyl)-2,4-dihydro-3*H*-1,2,4-triazol-3-one (5l): Light yellow solid; yield: 70%; m.p.: 156-157 ºC; ^{1}H NMR (500 MHz, chloroform-d_6) δ ppm: 11.58 (s, 1H), 9.06 (s, 1H), 8.12 (dt, *J* = 8.2, 1.5 Hz, 1H), 7.86 (t, *J* = 2.2 Hz, 1H), 7.76 (s, 1H), 7.58 (t, *J* = 8.2 Hz, 1H), 7.39 (ddd, *J* = 8.3, 2.2, 1.1 Hz, 1H). ^{13}C NMR (125 MHz, chloroform-d_6) δ ppm: 116.08, 121.01, 126.16, 128.11, 142.17, 147.54, 149.49, 150.73, 155.46. HRMS: *m/z*: For $C_9H_7N_5O_3$ ([M + H]$^+$): 234.0595, found 234.0591.

(*E*)-5-(((4-Aminophenyl)imino)methyl)-2,4-dihydro-3*H*-1,2,4-triazol-3-one (5m): White solid; yield: 78%; m.p.: 203-204 ºC; ^{1}H NMR (500 MHz, chloroform-d_6) δ ppm: 11.47 (s, 1H), 9.00 (s, 1H), 7.72 (s, 1H), 7.19 (d, *J* = 7.9 Hz, 2H), 6.61 (d, *J* = 7.9 Hz, 2H), 4.08 (s, 2H). ^{13}C NMR (125 MHz, chloroform-d_6) δ ppm: 115.48, 125.28, 139.73, 141.16, 144.64, 147.83, 153.48. HRMS: *m/z*: For $C_9H_9N_5O$ ([M + H]$^+$): 204.0793, found 204.0793.

(*E*)-5-(((4-(dimethylamino)phenyl)imino)methyl)-2,4-dihydro-3*H*-1,2,4-triazol-3-one (5n): White solid; yield: 78%; m.p.: 236-237 ºC; ^{1}H NMR (500 MHz, chloroform-d_6) δ ppm: 11.41 (s, 1H), 8.98 (s, 1H), 7.66 (s, 1H), 7.07 (d, *J* = 7.4 Hz, 2H), 6.72 (d, *J* = 7.3 Hz, 2H), 3.01 (s, 6H). ^{13}C NMR (125 MHz, chloroform-d_6) δ ppm: 41.57, 112.36, 125.18, 141.00, 142.89, 147.83, 150.73, 155.66. HRMS: *m/z*: For $C_{11}H_{13}N_5O$ ([M + H]$^+$): 232.1163, found 232.1159.

(*E*)-5-(((4-Hydroxyphenyl)imino)methyl)-2,4-dihydro-3*H*-1,2,4-triazol-3-one (5o): White solid; yield: 81%; m.p.: 188-189 ºC; ^{1}H NMR (500 MHz, chloroform-d_6) δ ppm: 11.51 (s, 1H), 9.02 (s, 1H), 7.74 (s, 1H), 7.66 (s, 1H), 7.20 (d, *J* = 8.5 Hz, 2H), 6.88 (d, *J* = 8.3 Hz, 2H). ^{13}C NMR (125 MHz, chloroform-d_6) δ ppm: 116.80, 125.16, 140.97, 143.81, 146.54, 154.61, 158.86. HRMS: *m/z*: For $C_9H_8N_4O_2$ ([M + H]$^+$): 205.0688, found 205.0684.

Molecular docking: The molecular docking studies were conducted [23] to investigate the binding interactions of novel compounds with the active sites of EGFR (PDB ID: 6LUD) and CDK-4 (PDB ID: 7SJ3). The docking procedures involved the following detailed steps:

Protein preparation: The X-ray crystal structures of EGFR and CDK-4 were retrieved from the Protein Data Bank. The protein structures were processed using Schrödinger's Protein Preparation Wizard. This step included the addition of hydrogen atoms, bond ordering and correction of any potential structural issues such as missing residues or incorrect bond assignments.

Ligand preparation: The 3D structures of the ligands were optimized using Schrödinger's LigPrep module, which utilized the OPLS 2005 force field. This module ensured proper geometry and stereochemistry of the ligands.

Grid box generation: For the docking simulations, the grid boxes were generated using Schrödinger's grid creation tool within Maestro 11.8. The grid boxes were centred on the active sites of the EGFR and CDK-4 proteins. The size of the grid boxes was adjusted to ensure full coverage of the binding sites, with dimensions set according to the spatial requirements of the ligands. Ligand-based constraints and positional restrictions were applied to focus the docking calculations on the relevant regions of the binding sites.

Docking protocol: Docking was performed using Glide's extra-precision (XP) mode. The genetic algorithm (GA) parameters included a specific number of GA steps to ensure comprehensive sampling of the conformational space. The docking parameters, including the number of solutions reported, were set to optimize the identification of potential binding conformations. Glide's scoring function, which incorporates electrostatic potential, strain, binding interactions and van der Waals energies, was employed to evaluate the binding affinity and pose quality of the docked compounds.

Scoring and analysis: The XP Glide score was used to assess the quality of ligand binding. This score is derived from a combination of factors including electrostatic interactions, van der Waals interactions and strain energies. The scoring function helps to rank the binding affinities of different ligand conformations and select the most promising candidates for further analysis.

MTT assay: The MTT assay was employed to assess the cytotoxicity and cell viability of synthesis of substituted 5-((phenylimino)methyl)-2,4-dihydro-3*H*-1,2,4-triazol-3-one (**5a-o**). Cultures of human cancer cell lines (HCT-116, A-549, PANC-1) were grown in 96-well plates and exposed to various concentrations (0.1 μM, 10 μM, 50 μM and 100 μM) of the compounds for 24-72 h. Following incubation, formazan crystals were produced by introducing MTT solution and then dissolved using DMSO. The quantification of absorbance was performed using a microplate reader in order to investigate the correlation between absorbance levels and cell viability. The reduced absorbance measurements indicated increased cytotoxicity and decreased cell viability. The results obtained from the MTT experiment, which involved varying concentrations and time periods, were utilized to determine the IC_{50} values of 1*H*-1,2,4-triazole-3-carboxamide derivatives for each cell line. The studies were performed three times and suitable controls were added to confirm the precision and dependability of the assay [24].

RESULTS AND DISCUSSION

The synthesis of substituted 5-((phenylimino)methyl)-2,4-dihydro-3*H*-1,2,4-triazol-3-one derivatives (**5a-o**) was successfully achieved through a multi-step process. The reaction began with the preparation of ethyl β-N-Boc-oxalamidrazone, followed by cyclization to form ethyl 5-oxo-4,5-dihydro-1*H*-1,2,4-triazole-3-carboxylate. Subsequent reduction yielded 5-oxo-4,5-dihydro-1*H*-1,2,4-triazole-3-carbaldehyde, which under-

went condensation with various substituted anilines to afford the final derivatives. The structures of the synthesized compounds were confirmed by spectroscopic techniques, including ^{1}H NMR, ^{13}C NMR and HRMS.

Molecular docking studies: Molecular docking experiments of designed imine-functionalized substituted 1,2,4-triazol-3-one derivatives against the two targets EGFR (6LUD) and CDK4 (7SJ3) revealed the broad range of binding affinities with the active sites of the compounds. The docking scores of the compounds are shown in Table-1.

TABLE-1
DOCKING SCORES OF IMINE-FUNCTIONALIZED SUBSTITUTED 1,2,4-TRIAZOL-3-ONE DERIVATIVES

Compd.	R	Docking score	
		6LUD	7SJ3
5a	H	-5.242	-5.923
5b	4-CH_3	-5.745	-6.028
5c	3-CH_3	-5.445	-6.363
5d	4-OCH_3	-6.323	-5.624
5e	4-F	-6.200	-5.908
5f	4-Cl	-5.873	-5.911
5g	4-Br	-5.785	-5.869
5h	4-CF_3	-6.286	-7.226
5i	3,4-$(CH_3)_2$	-6.155	-6.468
5j	3,4-$(OCH_3)_2$	-5.782	-6.450
5k	4-NO_2	-6.489	-6.123
5l	3-NO_2	-6.062	-6.357
5m	4-NH_2	-6.707	-6.099
5n	4-$N(CH_3)_2$	-6.623	-5.964
5o	4-OH	-6.797	-6.674

Molecular docking with EGFR (6LUD): The docking scores for 6LUD show a range between -5.2 and -6.8 with more negative values indicating stronger binding affinities. This suggests that certain substituents enhance interactions with the 6LUD binding site more effectively than others. Overall, the compounds with electron-withdrawing substituents such as -NO_2, -OH and -CF_3, tend to exhibit stronger binding. These groups likely contribute to the interaction by forming hydrogen bonds and electrostatic interactions within the binding pocket, thus stabilizing the complex.

The top-performing compounds for 6LUD include **5o** (4-OH), which achieved the highest docking score of -6.797, suggesting a strong affinity (Fig. 2). The hydroxyl group in **5o** likely facilitates hydrogen bonding, enhancing its stability with 6LUD. Other notable compounds include **5m** (4-NH_2) (Fig. 2) and **5k** (4-NO_2), with docking scores of -6.707 and -6.489, respectively. The amino and nitro groups in these compounds may engage in polar interactions, further improving their binding affinities. Moreover, compound **5h** (4-CF_3) shows a score of -6.286, benefitting from the electron-withdrawing properties of the -CF_3 group, which enhances hydrophobic and polar interactions within the 6LUD site.

The substituent analysis for 6LUD shows that electron-withdrawing groups, like 4-NO_2, 4-OH and 4-CF_3, are particularly effective for improving binding. In contrast, electron-donating groups such as 4-CH_3 (**5b**) and 3,4-$(CH_3)_2$ (**5i**) exhibit moderate scores of -5.745 and -6.155, respectively, possibly due to their limited polar interactions. Furthermore, positional isomerism appears to affect binding affinity; *para*-positioned substituents generally yield slightly better scores than their *meta* counterparts. For instance, **5k** (4-NO_2) scores -6.489 compared to **5l** (3-NO_2), which scores -6.062, suggesting that the *para* position aligns more favourably with 6LUD's binding site. Halogen substituents, like 4-F (**5e**), 4-Cl (**5f**) and 4-Br (**5g**), show moderate binding affinities, with fluorine performing best among them. These halogens might contribute to the interaction through hydrophobic contacts, though they lack the stronger polar effects seen with other substituents.

Molecular docking with CDK-4 (7SJ3): In case of 7SJ3, docking scores range from -5.6 to -7.2, generally indicating a stronger binding trend compared to 6LUD, suggesting that 7SJ3's binding pocket may favour certain substituents more.

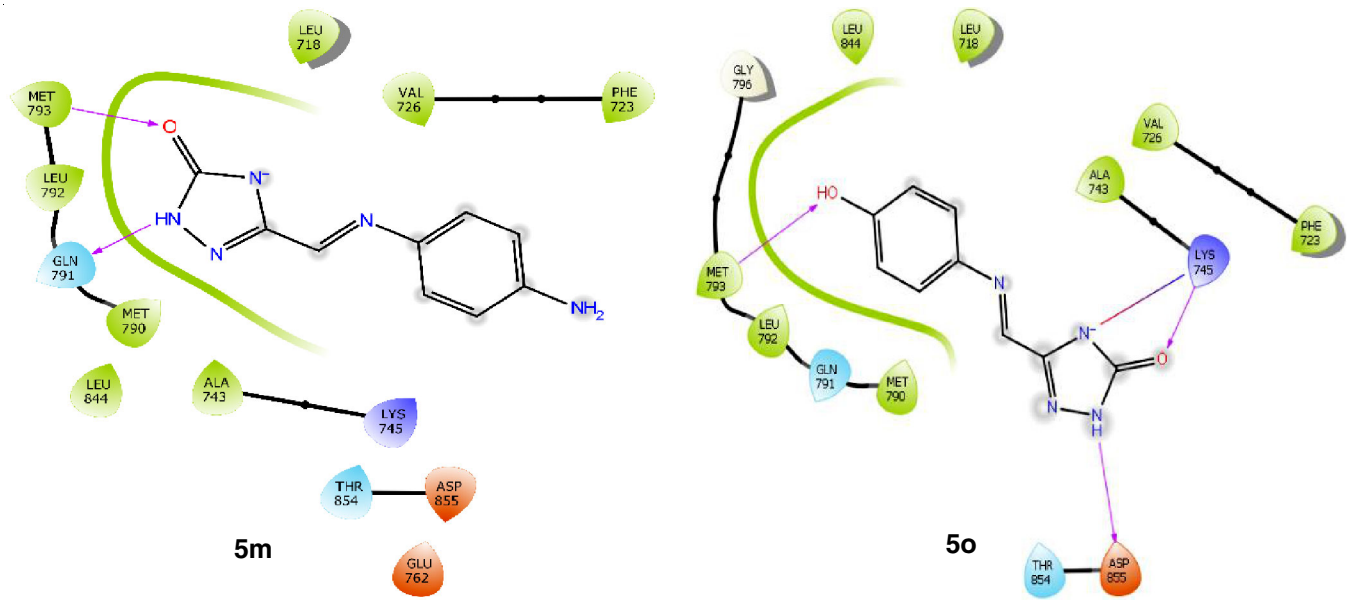

Fig. 2. Interactions of compounds **5m** and **5o** at the active site of 6LUD

Compounds with both electron-withdrawing and bulkier substituents, such as -CF_3, appear to have a particularly strong affinity for 7SJ3, highlighting a different interaction profile compared to 6LUD.

Among the top performers, **5h** (4-CF_3) has the strongest binding affinity, with a score of -7.226. The trifluoromethyl group likely supports hydrophobic interactions and van der Waals forces that are highly compatible with the 7SJ3 binding pocket (Fig. 3). **5o** (4-OH) also performs well, scoring -6.674, where the hydroxyl group likely forms hydrogen bonds with 7SJ3 (Fig. 3). Similarly, **5i** (3,4-$(CH_3)_2$) exhibits a strong score of -6.468, indicating that bulkier, hydrophobic substituents may be favoured by 7SJ3's binding environment.

The analysis of substituent effects on 7SJ3 suggests that, similar to 6LUD, electron-withdrawing groups such as -CF_3 and -NO_2 promote strong binding through polar and electrostatic interactions. The bulkier groups, like **5i** (3,4-$(CH_3)_2$) and **5j** (3,4-$(OCH_3)_2$), with scores of -6.468 and -6.45, respectively, show favourable interactions. This suggests that the 7SJ3 binding pocket may be more accommodating to larger groups that enhance van der Waals interactions and contribute to a tighter fit. Positional isomerism remains significant for 7SJ3, with *para*-substituted compounds generally showing better binding scores than their *meta* counterparts. For instance, **5k** (4-NO_2) has a score of -6.123, compared to **5l** (3-NO_2) at -6.357, likely due to better alignment with specific binding regions in 7SJ3. Halogenated compounds, including **5f** (4-Cl) and **5g** (4-Br), show moderate binding, with scores around -5.9. Unlike 6LUD, 7SJ3 appears to be less sensitive to differences among halogen substituents.

In summary, while both 6LUD and 7SJ3 show a preference for electron-withdrawing groups, they exhibit distinct interaction profiles. The 6LUD binding pocket favours smaller polar groups, such as -OH and -NO_2, for hydrogen bonding interactions. Conversely, the 7SJ3 pocket shows stronger affinity for bulkier and hydrophobic groups, such as -CF_3 and -CH_3 groups, which may better engage in van der Waals interactions. These findings highlight that while there are similarities in substituent preferences for each target, the specific binding environment of 7SJ3 allows it to accommodate larger groups more effectively than 6LUD.

Anticancer activity against non-small cell lung cancer (A549): The MTT assay results reveal the cytotoxicity of various imine-functionalized substituted 1,2,4-triazol-3-one derivatives against the A-549 non-small cell lung cancer cell line. The IC_{50} values (half-maximal inhibitory concentration) are presented as mean ± standard deviation, where lower IC_{50} values indicate higher potency of the compounds. The reference compound, doxorubicin, demonstrates a significantly lower IC_{50} value, affirming its well-established efficacy as a chemotherapeutic agent.

The most potent compounds (IC_{50} < 10 µM) include **5j** (3,4-$(OCH_3)_2$) with an IC_{50} of 5.96 ± 1.02 µM, **5h** (4-CF_3) at 7.80 ± 3.06 µM, **5m** (4-NH_2) at 8.08 ± 0.96 µM and **5o** (4-OH) at 8.85 ± 1.01 µM. Moderately potent compounds (10 µM ≤ IC_{50} < 15 µM) consist of **5i** (3,4-$(CH_3)_2$ at 9.88 ± 0.96 µM, **5c** (3-CH_3) at 10.56 ± 0.83 µM, **5b** (4-CH_3) at 14.50 ± 1.35 µM and others. The least potent compounds (IC_{50} ≥ 15 µM) include **5k** (4-NO_2) at 20.05 ± 2.34 µM, **5l** (3-NO_2) at 19.47 ± 1.01 µM and **5a** (H) at 15.84 ± 1.86 µM (Table-2).

The analysis of the effects of substituents on activity reveals notable trends. Compounds with electron-donating substituents (*e.g.* -CH_3, -OCH_3) generally exhibited better cytotoxicity than those with electron-withdrawing groups (*e.g.* -NO_2). For instance,

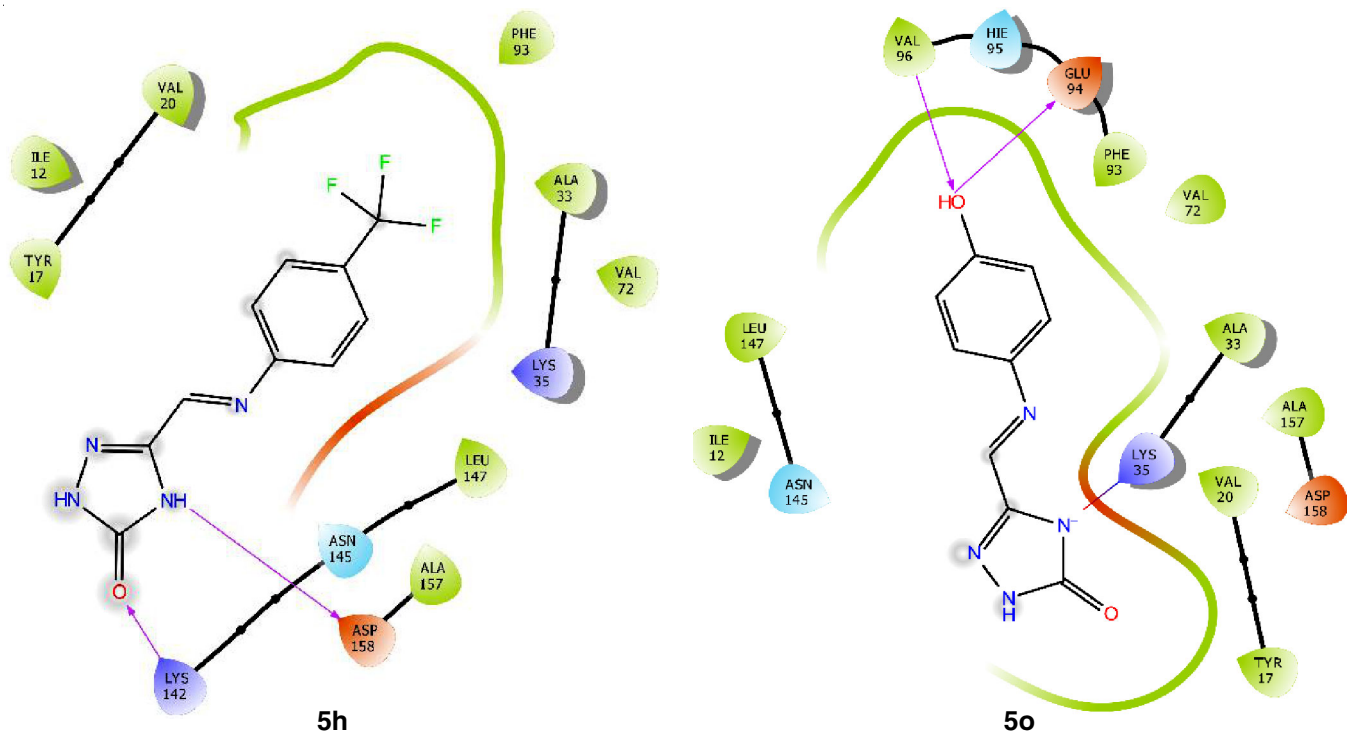

Fig. 3. Interactions of compounds **5h** and **5o** at the active site of 7SJ3

TABLE-2
IC_{50} VALUES OF SYNTHESIZED IMINE-FUNCTIONALIZED SUBSTITUTED 1,2,4-TRIAZOL-3-ONE DERIVATIVES

Compound	Non-small cell lung cancer line (A-549)	Colorectal cancer cell line (HCT-116)	Pancreatic cancer cell line (PANC-1)
5a	15.84 ± 1.86	24.64 ± 1.33	20.83 ± 2.38
5b	14.50 ± 1.35	18.94 ± 2.90	19.21 ± 3.20
5c	10.56 ± 0.83	16.90 ± 1.17	13.39 ± 1.67
5d	15.48 ± 1.92	21.23 ± 0.97	22.60 ± 0.97
5e	15.74 ± 1.15	23.37 ± 1.61	18.33 ± 1.86
5f	16.89 ± 1.06	18.52 ± 1.91	16.68 ± 1.02
5g	15.40 ± 0.96	16.76 ± 1.07	16.59 ± 2.45
5h	7.80 ± 3.06	9.54 ± 1.16	8.75 ± 1.86
5i	9.88 ± 0.96	11.54 ± 2.04	11.35 ± 2.73
5j	5.96 ± 1.02	7.12 ± 1.86	7.12 ± 1.86
5k	20.05 ± 2.34	15.44 ± 2.90	16.86 ± 3.28
5l	19.47 ± 1.01	16.25 ± 1.07	23.88 ± 1.52
5m	8.08 ± 0.96	9.06 ± 1.07	10.79 ± 2.45
5n	13.74 ± 1.86	10.87 ± 1.56	9.74 ± 2.38
5o	8.85 ± 1.01	9.79 ± 1.61	9.43 ± 1.52
Doxorubicin (ref. std)	1.14 ± 0.95	1.95 ± 0.56	1.74 ± 0.98

compound **5j** (3,4-$(OCH_3)_2$), which contains two methoxy groups, showed the lowest IC_{50} value of 5.96 ± 1.02 μM, indicating strong activity against A-549 cells. In contrast, compound **5k** (4-NO_2), with an electron-withdrawing nitro-substituent, exhibited the highest IC_{50} value of 20.05 ± 2.34 μM, suggesting reduced activity. The positioning of substituents significantly affects the compound's activity as well. For example, compound **5c** (3-CH_3) demonstrated an IC_{50} of 10.56 ± 0.83 μM, while compound **5b** (4-CH_3) had a slightly higher IC_{50} of 14.50 ± 1.35 μM. This indicates that the *meta*-positioned methyl group is more effective than the *para*-positioned methyl group in this context. Similarly, compound **5i** (3,4-$(CH_3)_2$), which has two methyl groups, exhibited favourable activity with an IC_{50} of 9.88 ± 0.96 μM, suggesting that substituents in close proximity may synergistically enhance activity.

Compounds containing hydrophilic groups such as -OH (**5o**) and -NH_2 (**5m**) also demonstrated promising results, with IC_{50} values of 8.85 ± 1.01 μM and 8.08 ± 0.96 μM, respectively. This suggests that hydrophilicity can enhance solubility and biological activity, potentially facilitating better interaction with target sites in cancer cells. When comparing the results with the reference compound doxorubicin, which demonstrated an IC_{50} of 1.14 ± 0.95 μM, it is evident that the tested derivatives show significant potential for further development. The activity of doxorubicin can be attributed to its ability to intercalate into DNA and inhibit topoisomerase II, leading to apoptosis in cancer cells. Notably, several derivatives, particularly **5j, 5h, 5m** and **5o**, exhibited encouraging activities that suggest their promising role in anticancer efficacy. These results warrant further exploration, including structural modifications and studies on their mechanisms of action.

These findings highlight the influence of substituents on the cytotoxic activity of imino-functionalized substituted 1,2,4-triazol-3-one derivatives against non-small cell lung cancer cells. Electron-donating and hydrophilic substituents enhance activity, while electron-withdrawing groups can impede efficacy. The structure-activity relationship elucidated in this study provides valuable insights for designing novel anticancer agents, underscoring the potential of optimizing substituent types and positions to improve therapeutic outcomes. Further investigations into the mechanisms underlying the observed cytotoxic effects are necessary to advance these compounds toward clinical relevance.

Anticancer activity against colorectal cancer cell line HCT-116: The MTT assay results indicate varying degrees of cytotoxicity among the tested imino functionalized substituted 1,2,4-triazol-3-one derivatives against the colorectal cancer cell line HCT-116. Compound **5h** (4-CF_3) emerged as the most potent derivative, exhibiting an IC_{50} of 9.54 ± 1.16 μM (Table-2). The presence of the trifluoromethyl group (-CF_3) likely enhances its lipophilicity and electronic properties, contributing to improved cell membrane permeability and interaction with intracellular targets. Similarly, **5j** (3,4-$(OCH_3)_2$) and **5m** (4-NH_2) also displayed significant activities, with IC_{50} values of 7.12 ± 1.86 μM and 9.06 ± 1.07 μM, respectively. The presence of methoxy and amino groups may facilitate hydrogen bonding and enhance the binding affinity to biological targets, increasing their anticancer potential.

Compounds such as **5b** (4-CH_3), **5d** (4-OCH_3) and **5f** (4-Cl) exhibited moderate activity, with IC_{50} values ranging from 18.52 ± 1.91 μM to 21.23 ± 0.97 μM. These derivatives suggest that while they possess some efficacy, there is substantial room for improvement through structural modifications. The presence of methyl (-CH_3), methoxy (-OCH_3) and chloro (-Cl) groups may influence the overall activity by affecting electronic distribution, although the impacts appear less pronounced compared to the more potent compounds.

On the other hand, derivatives such as **5a** (H) and **5e** (4-F) showed the highest IC_{50} values at 24.64 ± 1.33 μM and 23.37 ± 1.61 μM, respectively. This suggests that these compounds are less effective in inhibiting the growth of HCT-116 cells. The hydrogen (H) and fluoro (F) substituents may not provide sufficient interaction with the target, leading to diminished potency, as the lack of more complex functional groups that enhance binding may account for their lower activity levels.

In comparison to doxorubicin, the activities of the derivatives illustrate varying potentials for anticancer effects. While the derivatives show higher IC_{50} values, the promising activities of compounds like **5h**, **5j** and **5m** indicate that they could be further optimized to enhance their potency (Fig. 4). The results warrant further exploration of the most promising compounds, particularly **5h**, **5j** and **5m**, through additional structural modifications.

Anticancer activity against pancreatic cancer cell line PANC-1: The MTT assay results for the imino functionalized substituted 1,2,4-triazol-3-one derivatives (**5a-o**) against the pancreatic cancer cell line PANC-1 reveal varying levels of cytotoxicity. The reference compound doxorubicin demonstrated a potent IC_{50} value of 1.74 ± 0.98 μM, serving as a benchmark for evaluating the efficacy of the tested derivatives.

Among the tested compounds, **5h** (4-CF_3) exhibited the most promising activity with an IC_{50} of 8.75 ± 1.86 μM. The

trifluoromethyl group (CF_3) may enhance the lipophilicity and electron-withdrawing capacity of the compound, potentially increasing its binding affinity to biological targets involved in cancer cell proliferation. Similarly, **5j** (3,4-$(OCH_3)_2$) also showed significant activity with an IC_{50} of 7.12 ± 1.86 µM, suggesting that the presence of methoxy groups may facilitate better interactions with the target, possibly through hydrogen bonding or dipole-dipole interactions.

Compounds **5m** (4-NH_2), **5n** (4-$N(CH_3)_2$) and **5o** (4-OH) exhibited moderate activity with IC_{50} values of 10.79 ± 2.45 µM, 9.74 ± 2.38 µM and 9.43 ± 1.52 µM, respectively (Table-2). The amino (-NH_2), dimethylamino (-$N(CH_3)_2$) and hydroxyl (-OH) substituents appear to contribute positively to the anticancer activity, indicating that these functional groups may enhance solubility and increase the compound's ability to penetrate cell membranes, thus facilitating their therapeutic effects.

In contrast, derivatives such as **5l** (3-NO_2) and **5d** (4-OCH_3) displayed the least potency with IC_{50} values of **2**3.88 ± 1.52 µM and 22.60 ± 0.97 µM, respectively. The presence of nitro (-NO_2) and methoxy (-OCH_3) groups in these positions may not effectively enhance the interaction with the target, potentially due to steric hindrance or unfavourable electronic effects that reduce their overall activity. Other compounds, including **5e** (4-F), **5f** (4-Cl) and **5g** (4-Br), also demonstrated moderate cytotoxicity, with IC_{50} values ranging from 16.59 ± 2.45 µM to 18.33 ± 1.86 µM. The halogen substituents (F, Cl and Br) may impart varying electronic properties, although their impact on overall activity appears less effective compared to the more potent compounds.

The results illustrate a clear distinction in the anticancer activities of the tested derivatives compared to doxorubicin (Fig. 4). Overall, the analysis indicates that certain substituents, particularly -CF_3 and -OCH_3, significantly enhance the anticancer activity of the derivatives against PANC-1 cells. Future work should focus on optimizing the most promising compounds, such as **5h** and **5j**, through structural modifications and indepth studies of their mechanisms of action. Exploring different substitution patterns and incorporating additional functional groups may yield derivatives with improved efficacy against pancreatic cancer.

Conclusion

The synthesized imine-functionalized substituted 1,2,4-triazol-3-one derivatives (**5a-o**) were successfully obtained through a multistep synthetic route, as confirmed by spectral and physico-chemical characterization. Molecular docking studies against EGFR (6LUD) and CDK4 (7SJ3) identified significant binding affinities, particularly for compounds bearing electron-withdrawing (-CF_3, -NO_2, -OH) and hydrophobic (-CH_3) groups. Notably, compound **5o** demonstrated the highest affinity for EGFR (-6.797), while **5h** exhibited the strongest interaction with CDK4 (-7.226), underscoring their potential as selective inhibitors. The anticancer evaluation against three cell lines (A549, HCT-116 and PANC-1) highlighted several promising leads. In the HCT-116 colorectal cancer cell line, compound **5h** (4-CF_3) displayed the highest potency with an IC_{50} value of 6.24 ± 0.78 µM, followed by **5j** (3,4-$(OCH_3)_2$) and **5o** (4-OH) with IC_{50} values of 7.50 ± 1.05 µM and 8.31 ± 0.92 µM, respectively. For PANC-1 pancreatic cancer cells, compound **5j** emerged as the most effective, with an IC_{50} of 5.96 ± 1.02 µM, followed by **5h** and **5m** (4-NH_2), with IC_{50} values of 7.80 ± 3.06 µM and 8.08 ± 0.96 µM, respectively. The structure-activity relationship analysis revealed that electron-donating groups, such as -OCH_3 and -CH_3, enhanced cytotoxicity across all cell lines, whereas electron-withdrawing groups like -NO_2 showed reduced activity. Furthermore, *para*-substituted derivatives generally demonstrated superior efficacy compared to their *meta*-substituted counterparts, emphasizing the importance of substituent positioning. These findings demonstrate the therapeutic potential of imine-functionalized substituted 1,2,4-triazol-3-one derivatives as anticancer agents, warranting further investigations to optimize their efficacy and selectivity.

ACKNOWLEDGEMENTS

The authors are grateful to the Department of Chemistry, Andhra University, Vishakhapatnam, India, for providing the critical support in completing the current work.

CONFLICT OF INTEREST

The authors declare that there is no conflict of interests regarding the publication of this article.

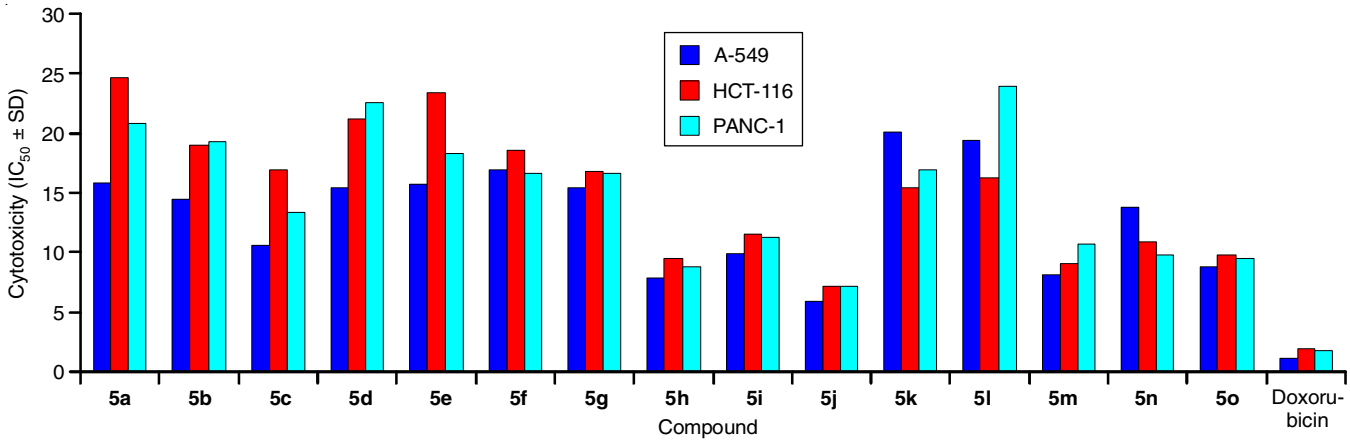

Fig. 4. IC_{50} values comparison of compounds **5a-o** across all the tested cell lines

REFERENCES

1. H. Mithoowani and M. Febbraro, *Curr. Oncol.*, **29**, 1828 (2022); https://doi.org/10.3390/curroncol29030150
2. U. Anand, A. Dey, A.K.S. Chandel, R. Sanyal, A. Mishra, D.K. Pandey, V. De Falco, A. Upadhyay, R. Kandimalla, A. Chaudhary, J.K. Dhanjal, S. Dewanjee, J. Vallamkondu and J.M. Pérez De La Lastra, *Genes Dis.*, **10**, 1367 (2023); https://doi.org/10.1016/j.gendis.2022.02.007
3. W.M.C. Van Den Boogaard, D.S.J. Komninos and W.P. Vermeij, *Cancers*, **14**, 627 (2022); https://doi.org/10.3390/cancers14030627
4. R. Kaur, A.R. Dwivedi, B. Kumar and V. Kumar, *Anticancer. Agents Med. Chem.*, **16**, 465 (2016); https://doi.org/10.2174/1871520615666150819121106
5. E. Bonandi, M.S. Christodoulou, G. Fumagalli, D. Perdicchia, G. Rastelli and D. Passarella, *Drug Discov. Today*, **22**, 1572 (2017); https://doi.org/10.1016/j.drudis.2017.05.014
6. J. Murray, O.E. Young, L. Renshaw, S. White, L. Williams, D.B. Evans, J.M. Thomas, M. Dowsett and J.M. Dixon, *Breast Cancer Res. Treat.*, **114**, 495 (2009); https://doi.org/10.1007/s10549-008-0027-0
7. S.A. Shahzad, M. Yar, Z.A. Khan, L. Shahzadi, S.A.R. Naqvi, A. Mahmood, S. Ullah, A.J. Shaikh, T.A. Sherazi, A.T. Bale, J. Kuku³owicz and M. Bajda, *Bioorg. Chem.*, **85**, 209 (2019); https://doi.org/10.1016/j.bioorg.2019.01.005
8. H. Bera, B.J. Tan, L. Sun, A.V. Dolzhenko, W.-K. Chui and G.N.C. Chiu, *Eur. J. Med. Chem.*, **67**, 325 (2013); https://doi.org/10.1016/j.ejmech.2013.06.051
9. Z. Song, Y. Liu, Z. Dai, W. Liu, K. Zhao, T. Zhang, Y. Hu, X. Zhang and Y. Dai, *Bioorg. Med. Chem.*, **24**, 4723 (2016); https://doi.org/10.1016/j.bmc.2016.08.014
10. R.Z. Batran, D.H. Dawood, S.A. El-Seginy, M.M. Ali, T.J. Maher, K.S. Gugnani and A.N. Rondon-Ortiz, *Arch. Pharm.*, **350**, 1700064 (2017); https://doi.org/10.1002/ardp.201700064
11. M. Qin, S. Yan, L. Wang, H. Zhang, Y. Zhao, S. Wu, D. Wu and P. Gong, *Eur. J. Med. Chem.*, **115**, 1 (2016); https://doi.org/10.1016/j.ejmech.2016.02.071
12. J. Liu, M. Nie, Y. Wang, J. Hu, F. Zhang, Y. Gao, Y. Liu and P. Gong, *Eur. J. Med. Chem.*, **123**, 431 (2016); https://doi.org/10.1016/j.ejmech.2016.07.059
13. M.I. Han, H. Bekçi, A.I. Uba, Y. Yildirim, E. Karasulu, A. Cumaoglu, H.Y. Karasulu, K. Yelekçi, Ö. Yilmaz and S.G. Küçükgüzel, *Arch. Pharm. (Weinheim)*, **352**, 1800365 (2019); https://doi.org/10.1002/ardp.201800365
14. I.H. Eissa, A.M. Metwaly, A. Belal, A.B.M. Mehany, R.R. Ayyad, K. El-Adl, H.A. Mahdy, M.S. Taghour, K.M.A. El-Gamal, M.E. El-Sawah, S.A. Elmetwally, M.A. Elhendawy, M.M. Radwan and M.A. ElSohly, *Arch. Pharm.*, **352**, 1900123 (2019); https://doi.org/10.1002/ardp.201900123
15. M.K. Ibrahim, M.S. Taghour, A.M. Metwaly, A. Belal, A.B.M. Mehany, M.A. Elhendawy, M.M. Radwan, A.M. Yassin, N.M. El-Deeb, E.E. Hafez, M.A. ElSohly and I.H. Eissa, *Eur. J. Med. Chem.*, **155**, 117 (2018); https://doi.org/10.1016/j.ejmech.2018.06.004
16. G. Sáez-Calvo, A. Sharma, F.D.A. Balaguer, I. Barasoain, J. Rodríguez-Salarichs, N. Olieric, H. Muñoz-Hernández, S. Wendeborn, M.A. Peñalva, M.Á. Berbís, R. Matesanz, Á. Canales, J.M. Jímenez-Barbero, A.E. Prota, J.M. Andreu, C. Lamberth, M.O. Steinmetz and J.F. Díaz, *Cell Chem. Biol.*, **24**, 737 (2017); https://doi.org/10.1016/j.chembiol.2017.05.016
17. M. Alswah, A. Bayoumi, K. Elgamal, A. Elmorsy, S. Ihmaid and H. Ahmed, *Molecules*, **23**, 48 (2017); https://doi.org/10.3390/molecules23010048
18. M. Szumilak, A. Wiktorowska-Owczarek and A. Stanczak, *Molecules*, **26**, 2601 (2021); https://doi.org/10.3390/molecules26092601
19. N. Li, C. Chen, H. Zhu, Z. Shi, J. Sun and L. Chen, *Bioorg. Chem.*, **111**, 104867 (2021); https://doi.org/10.1016/j.bioorg.2021.104867
20. L.E. Grebenkina, A.V. Matveev and M.V. Chudinov, *Chem. Heterocycl. Compd.*, **56**, 1173 (2020); https://doi.org/10.1007/s10593-020-02794-2
21. D. Webb and T.F. Jamison, *Org. Lett.*, **14**, 568 (2012); https://doi.org/10.1021/ol2031872
22. S. Morales, F.G. Guijarro, J.L. García Ruano and M.B. Cid, *J. Am. Chem. Soc.*, **136**, 1082 (2014); https://doi.org/10.1021/ja4111418
23. B.J. Bender, S. Gahbauer, A. Luttens, J. Lyu, C.M. Webb, R.M. Stein, E.A. Fink, T.E. Balius, J. Carlsson, J.J. Irwin and B.K. Shoichet, *Nat. Protoc.*, **16**, 4799 (2021); https://doi.org/10.1038/s41596-021-00597-z
24. T.L. Riss, R.A. Moravec, A.L. Niles, S. Duellman, H.A. Benink, T.J. Worzella and L. Minor, in eds.: S. Markossian, A. Grossman, H. Baskir, M. Arkin, D. Auld, C. Austin, J. Baell, K. Brimacombe, T.D.Y. Chung, N.P. Coussens, J.L. Dahlin, V. Devanarayan, T.L. Foley, M. Glicksman, K. Gorshkov, S. Grotegut, M.D. Hall, S. Hoare, J. Inglese, P.W. Iversen, M. Lal-Nag, Z. Li, J.R. Manro, J. McGee, A. Norvil, M. Pearson, T. Riss, P. Saradjian, G.S. Sittampalam, M.A. Tarselli, O.J. Trask Jr., J.R. Weidner, M.J. Wildey, K. Wilson, M. Xia and X. Xu, Cell Viability Assays, In: Assay Guidance Manual, Eli Lilly & Company and the National Center for Advancing Translational Sciences, Bethesda, MD (2004).